

The Origin and Chemical Evolution of the Exotic Globular Cluster NGC3201

C. Muñoz ^{*}, D. Geisler and S. Villanova

Departamento de Astronomía, Casilla 160-C, Universidad de Concepción, Concepción, Chile

28 August 2018

ABSTRACT

NGC3201 is a globular cluster (GC) which shows very peculiar kinematic characteristics including an extreme radial velocity and a highly retrograde orbit, strongly suggesting an extraGalactic origin.

Our aims are to study NGC3201 in the context of multiple populations (MPs), hoping to constrain possible candidates for the self-enrichment by studying the chemical abundance pattern, as well as adding insight into the origin of this intriguing cluster.

We present a detailed chemical abundance analysis of eight red giant branch (RGB) stars using high resolution spectroscopy. We measured 29 elements and found $[\text{Fe}/\text{H}] = -1.53 \pm 0.01$, we cannot rule out a metallicity spread of ~ 0.12 dex, and an α -enhancement typical of halo GCs. However significant spreads are observed in the abundances of all light elements except for Mg. We confirm the presence of an extended Na-O anticorrelation. n-capture elements generally are dominated by the r-process, in good agreement with the bulk of Galactic GCs. The total (C+N+O) abundance is slightly supersolar and requires a small downward correction to the isochrone age, yielding 11.4 Gyr.

Kinematically, NGC3201 appears likely to have had an extraGalactic origin but its chemical evolution is similar to most other, presumably native, Galactic GCs.

Key words: Galaxy: Globular Cluster:individual: NGC3201 - stars: abundances

1 INTRODUCTION

GCs are of paramount importance in the investigation of a wide variety of fundamental astrophysical phenomena. They are the perfect laboratories for studying a wide variety of fundamental problems in stellar and galactic astrophysics. Our knowledge of stellar evolution is grounded in the detailed comparison of GC color-magnitude diagrams with model isochrones. They are the oldest objects known whose ages are relatively easily and accurately measured, setting a firm lower limit to the age of the Universe.

Only a few years ago GCs, with the lone exception of ω Cen, were considered Simple Stellar Populations, with all stars in a cluster believed to share the same age and chemical composition. This simplicity has been shattered by the discovery of increasing complexity in the latter parameter for a growing number of GCs, spawning the new and exciting field of multiple populations (MPs). Both photometric and spectroscopic techniques are employed to trace and understand this phenomenon. The development of larger tele-

scopes, more sensitive detectors and high resolution multi-object spectrographs has allowed a large sample of giants in each of a growing number of GCs to be studied with high resolution spectroscopy, leading to an ever-increasing database of elemental abundances. The emerging picture, although quite complicated in detail, does show several salient features.

In particular, light elements (C, N, O, Na, Mg, Al) are associated with the MP phenomenon. The most typical and best-studied characteristic is the Na-O anticorrelation. Indeed, the ubiquity of this anticorrelation in their sample of 19 GCs studied prompted Carretta et al. (2009a,b) to introduce a new, chemical definition of a GC as those objects which exhibit such a feature. This spread in the light elements must be due to self-enrichment that happens within a GC in the early stages of its formation, when a second generation of stars was born from gas polluted by ejecta of evolved stars of the first generation (Caloi & D’Antona 2011). Several kinds of polluters for the light elements have been proposed: intermediate mass AGB stars (D’Antona et al. 2002), fast rotating massive MS stars (Decressin et al. 2007) and massive binaries (de Mink et al. 2010). In addi-

^{*} cesarmunoz@astro-udec.cl

tion, a few of the most massive clusters such as ω Cen (Johnson et al. 2008; Marino et al. 2011a), M54 (Carretta et al. 2010b) and M22 (Marino et al. 2011b) are now known to show significant spreads in Fe as well. Indeed, the existence of such a metallicity spread has also been claimed in NGC3201 (Gonzalez & Wallerstein 1998; Simmerer et al. 2013), but remains controversial. Such clusters must also have been able to retain SNeII and/or SNeIa ejecta (Marcolini et al. 2009), as well as material ejected from polluters at lower velocity which led to the Na-O anticorrelation. Ejecta from evolved stars (cycled through a temperature of $T > 10^7$ K where hot H-burning occurs) is returned to the interstellar medium of the GC and mixes with the remaining primordial gas left over from the first star formation epoch. Given a sufficiently deep potential well to retain this ejecta, which is the critical parameter, a second generation of star formation can occur once the appropriate conditions arise (e.g. Cottrell & Da Costa 1981; Carretta et al. 2010c).

NGC3201 is unique among the Galactic GCs kinematically. It has the most extreme radial velocity (495 km s^{-1}). Gonzalez & Wallerstein (1998) calculated an orbital velocity of 250 km s^{-1} around the Galactic center, but in a retrograde sense. This has been taken as strong evidence of a possible extraGalactic formation with subsequent capture by the MW (Rodgers & Paltoglou 1984; van den Bergh 1993).

Examining the color-magnitude diagram (CMD) of NGC3201 (e.g. Layden & Sarajedini 2003) clearly shows that it has a very populated and extended horizontal branch (HB). According to D’Antona et al. (2002), the extension of the HB in a GC is proportional to the amount of helium variation due to self-pollution among its stars. Therefore, the large extension of the HB in NGC3201 suggests that it should display a large spread in the light elements.

Kravtsov et al. (2009) and Carretta et al. (2010d) found radial inhomogeneities in the stellar populations of NGC3201, Kravtsov found radial variations in the CMD, that could not be explained by reddening. Carretta et al. (2010d) compared their spectroscopic sample of 100 stars with Na and O abundances with photometric data and found that the giant stars of the second generation have a tendency to be more concentrated than stars of the first generation, as expected in the self-pollution scenario.

Several chemical analyses have been carried out on NGC 3201 stars using high-resolution spectroscopy. Unfortunately, these are not sufficient to give a definitive picture of the chemical evolution of this interesting GC. Gonzalez & Wallerstein (1998) measured the abundances of several chemical elements in eighteen stars but with large errors, based on CTIO 4m data. Carretta et al. (2009a) observed a large sample of some 100 stars but only measured the abundances of light elements (O, Na, Mg, Al and Si), as well as Fe. Simmerer et al. (2013) observed a sample of 24 stars but only measured Fe. They found an intrinsic spread in iron. We discuss this point in detail in section 4.1. Our sample (only eight stars), although much smaller than either the Gonzalez, Carretta or Simmerer samples, was observed with high resolution as well as excellent signal to noise (see section 2), which allows us to measure the abundances of more elements (29 total) with much smaller errors than in the previous studies.

In Section 2 we describe the data reduction and

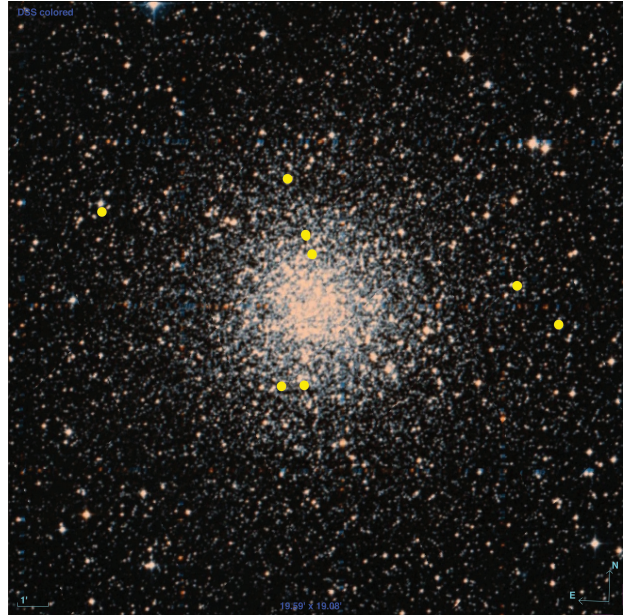


Figure 1. The spatial distribution of the stars observed (yellow filled circles) in NGC3201. (picture from SDSS).

in Section 3 the methodology we used to obtain the chemical abundances. In Section 4 we present our results including iron-peak elements, alpha elements, the Na-O anti-correlation, the Mg-Al anti-correlation, the total (C+N+O) abundance, the correction to age estimates due to the former, and heavy elements. In Section 5 we discuss the origin of NGC3201. Finally in Section 6 we give a summary of our main findings.

2 OBSERVATIONS AND DATA REDUCTION

Our dataset consists of high resolution spectra obtained with the MIKE spectrograph mounted on the Magellan Clay telescope at Las Campanas Observatory, collected in March 2011. Our targets include 9 stars between $K=8.6$ and $K=9.8$ selected from the upper RGB. Our selection criteria included an attempt to cover a wide spatial distribution around the GC (see Figures 1 and 2). Each star was observed with the blue and red arms of the spectrograph, and spectra cover a wide range from 3900-8079 Å with a resolving power of $R \sim 41,000$ in the blue and $R \sim 32,000$ in the red. Exposure times were between 240-600 seconds. For some giants, we stacked several spectra in order to increment the S/N. The S/N is between 40-90 at 6500 Å.

Data were reduced using a pipeline from LCO for this instrument (<http://code.obs.carnegiescience.edu/mike>). Data reduction includes bias subtraction, flat-field correction, wavelength calibration, sky subtraction, and spectral rectification.

We measured radial velocities using the fxcor package in IRAF and a synthetic spectrum as a template. This spectrum was generated using the mean of the atmospheric parameters of our stars. One star (0437-0223437 NOMAD-1 Catalog) shows a very discrepant radial velocity (20.76 km s^{-1}), and so was rejected as a non-member. The mean heliocentric radial velocity value for our remaining 8 targets is $495.18 \pm 0.81 \text{ km s}^{-1}$, while the dispersion is 2.14 km

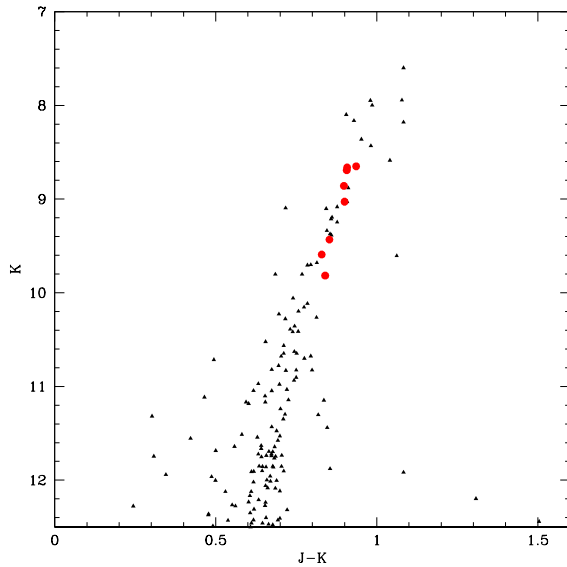


Figure 2. The CMD of NGC3201 from NOMAD catalogue (Zacharias et al. 2004) with the observed RGB stars indicated as red filled circles.

s^{-1} . The mean radial velocity is in excellent agreement with the values in the literature: Carretta et al. (2009a) found a value of $494.57 \pm 1.07 \text{ km s}^{-1}$ and Harris (1996) quote a value of $494 \pm 0.2 \text{ km s}^{-1}$. Table 1 lists the basic parameters of the selected stars: ID (the NOMAD-1 Catalog), the J2000 coordinates (RA and Dec), V, B magnitudes (Cote et al. 1994), K, J magnitudes (2MASS), heliocentric radial velocity, T_{eff} , $\log(g)$, micro-turbulent velocity (v_t) and metallicity ([Fe/H]).

3 ABUNDANCE ANALYSIS

The chemical abundances for Ca, Ti, Cr, Fe and Ni were obtained using equivalent widths (EWs) of the spectral lines. See Marino et al. (2008) for a more detailed explanation of the method we used to measure the EWs. For the other elements (C, N, O, Na, Mg, Al, Si, Sc, V, Mn, Co, Cu, Zn, Y, Zr, Ba, La, Ce, Pr, Nd, Sm, Eu, Dy, Pb), whose lines are affected by blending, we used the spectrum-synthesis method. We calculated 5 synthetic spectra having different abundances for each line, and estimated the best-fitting value as the one that minimizes the rms scatter. Only lines not contaminated by telluric lines were used.

Atmospheric parameters were obtained in the following way. First, T_{eff} was derived from the B-V color (Cote et al. 1994) using the relation of Alonso et al. (1999) and the reddening ($E(B-V)=0.24$) from Harris (1996). Surface gravities ($\log(g)$) were obtained from the canonical equation:

$$\log(g/g_{\odot}) = \log(M/M_{\odot}) + 4\log(T_{eff}/T_{\odot}) - \log(L/L_{\odot})$$

Where the mass was assumed to be $0.8 M_{\odot}$, and the luminosity was obtained from the absolute magnitude M_v , assuming an apparent distance modulus of $(m-M)_v = 14.20$ (Har-

ris 1996). The bolometric correction (BC) was derived by adopting the $BC:T_{eff}$ relation from Alonso et al. (1999). Finally, the micro-turbulent velocity (v_t) was obtained from the relation of Marino et al. (2008). These atmospheric parameters were taken as initial estimates and were refined during the abundance analysis. As a first step, atmospheric models were calculated using ATLAS9 (Kurucz 1970) and assuming the initial estimate of T_{eff} , $\log(g)$, v_t , and the [Fe/H] value from Harris (1996). Then T_{eff} , v_t , and $\log(g)$ were adjusted and new atmospheric models calculated iteratively in order to remove trends in excitation potential and equivalent width vs. abundance for T_{eff} and v_t respectively, and to satisfy the ionization equilibrium for $\log(g)$. FeI and FeII were used for this latter purpose. The [Fe/H] value of the model was changed at each iteration according to the output of the abundance analysis. The local Thermodynamic Equilibrium (LTE) program MOOG (Snedden 1973) was used for the abundance analysis. The linelist for the chemical analysis was described in previous papers (e.g. Villanova & Geisler 2011). The adopted solar abundances we used are reported in Table 2.

Abundances for C, N and O were determined all together interactively in order to take into account molecular coupling of these elements. Our targets are objects evolved off the main sequence, so some evolutionary mixing is expected. This can affect the primordial C, N and O abundances separately, but should not affect the total (C+N+O) content because these elements are transformed one into the other during the CNO cycle. Since all of our stars are in the same evolutionary phase, relative C, N, O abundances should also be unaffected.

An internal error analysis was performed by varying T_{eff} , $\log(g)$, [Fe/H], and v_t and redetermining abundances of star #0436-0222665, assumed to be representative of the entire sample. Parameters were varied by $\Delta T_{eff} = +40 \text{ K}$, $\Delta \log(g)=+0.14$, $\Delta[\text{Fe}/\text{H}]=+0.05 \text{ dex}$, and $\Delta v_t = +0.03 \text{ km s}^{-1}$, which we estimated as our internal errors. This estimation of the internal errors for the atmospheric parameters was performed as in Marino et al. (2008). Results are given in Table 3, including the error due to the noise of the spectra. This error was obtained as the average value of the errors of the mean given by MOOG for elements measured via EQW; and for elements whose abundance was obtained by spectrum-synthesis, as the error given by the fitting procedure. σ_{tot} is the squareroot of the sum of the squares of the individual errors, while σ_{obs} is the mean observed dispersion. The light elements C, N, O, Na and Al show a large excess of σ_{obs} over σ_{tot} , indicating inhomogeneity for these elements. For all other elements except Dy, the agreement is good, indicating no significant intrinsic spread.

In the case of Sr our measurements give an abundance which is very low, using the line at 4607.33 \AA . In the literature, several other lines have been used to measure Sr, e.g. 4077.71 \AA and 4215.5 \AA . However, these lines have problems due to the large noise present in that part of our spectra. Bergemann et al. (2012) and Hansen et al. (2013) found that the 4607.33 \AA line gave widely varying results when compared with the line usually used (4077.71 \AA) using an LTE model. Because of this, we decided to not use the values of Sr.

The abundance of [Na/Fe] was corrected by -0.05 dex using

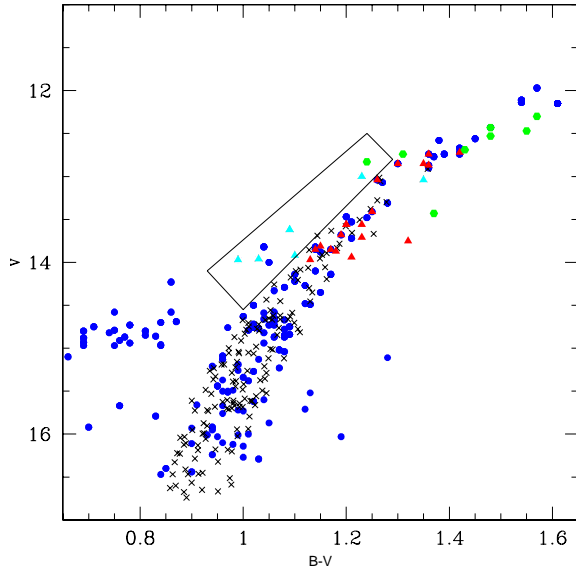


Figure 3. The CMD of NGC3201, filled green circles are our data, filled blue circles are data from Cote et al. (1994), black crosses are data from Carretta et al. (2009c), red filled triangles are data from Simmerer et al. (2013) with $[\text{Fe}/\text{H}] \geq -1.56$ and cyan filled triangles are data from Simmerer et al. (2013) with $[\text{Fe}/\text{H}] \leq -1.59$.

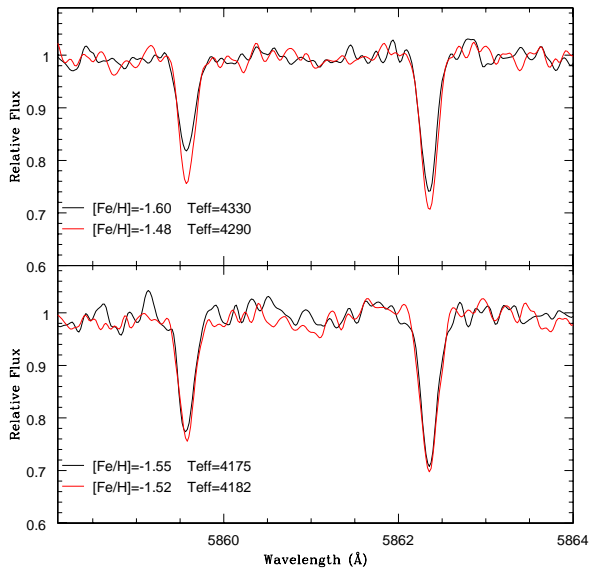


Figure 4. The upper panel shows the spectral comparison between our most metal-poor star #3 and our most metal-rich star #4 in two lines of Fe. The bottom panel shows the comparison between stars #6 y #7, both with similar $[\text{Fe}/\text{H}]$ and temperature, for the same Fe lines.

the non-LTE (NLTE) correction (constant for our range of temperature) from Mashonkina et al. (2000). For all other elements the selected lines should not be affected significantly by NLTE.

3.1 Reddening

The reddening in NGC3201 is a factor to consider given its low galactic latitude ($b = 8.6^\circ$). The nominal color excess is $E(B-V) = 0.24$ (Harris 1996), but a significant differential reddening exists. Gonzalez & Wallerstein (1998) reported a variation in reddening of about 0.1 mag in E_{B-V} . von Braun & Mateo (2001) found a differential reddening of 0.2 mag in E_{V-I} .

Although, initially, the atmospheric parameters were determined using the nominal reddening, and are thus susceptible to error due to the differential reddening of this cluster, these parameters were refined interactively, presumably thereby minimizing the effects of reddening on the measurement of abundances.

4 RESULTS

In the following section, we discuss in detail our results and compare them with the literature.

4.1 Iron-peak elements

We found a mean $[\text{Fe}/\text{H}]$ value for NGC3201 of:

$$[\text{Fe}/\text{H}] = -1.53 \pm 0.01 \text{ dex}$$

The observed scatter is entirely consistent with that expected solely from errors and thus we find no evidence for any intrinsic Fe abundance spread, except for star 3 of our sample (analyzed in more detail below). Gonzalez & Wallerstein (1998) found a mean $[\text{Fe}/\text{H}] = -1.42 \pm 0.12$ from their high resolution analysis of eighteen stars. Some of their stars showed Fe abundances significantly different from the mean, but they associated this behavior as likely due to a systematic error in the abundance determination and not a real metallicity spread. Although Covey et al. (2003) cannot confirm a spread of iron in NGC 3201 greater than 0.3 dex. Carretta et al. (2009c) used GIRAFFE at the VLT to obtain high resolution spectra for 149 giants. They found a mean $[\text{Fe}/\text{H}] = -1.50 \pm 0.07$ with $\sigma = 0.049$. In addition, their sample of 13 even higher resolution UVES stars yielded a mean $[\text{Fe}/\text{H}] = -1.51 \pm 0.08$ with $\sigma = 0.07$. Their combined sample is impressively large and homogeneously analyzed and they did not find any spread. The results from Carretta are in excellent agreement with ours, both in mean $[\text{Fe}/\text{H}]$ as well as the lack of an Fe abundance spread, giving us added confidence in our results.

On the other hand, Simmerer et al. (2013) recently found an intrinsic spread of iron of 0.4 dex in a sample of 24 RGB stars. However, when we analyze the photometry of the metal poor stars from Simmerer et al. (2013), we see that 5 of the 6 stars with $[\text{Fe}/\text{H}] \leq -1.59$ (filled cyan triangles in Figure 3) are most likely AGB and not RGB stars, as shown in Figure 3. Stars with $[\text{Fe}/\text{H}] \geq -1.56$ from Simmerer et al. (2013) are essentially all RGB stars.

It is noteworthy that when comparing the 149 stars from Carretta et al. (2009c) with the data from Cote et al. (1994), which cover the full color range of the RGB, we note that Carretta covered RGB fairly well, giving reliability

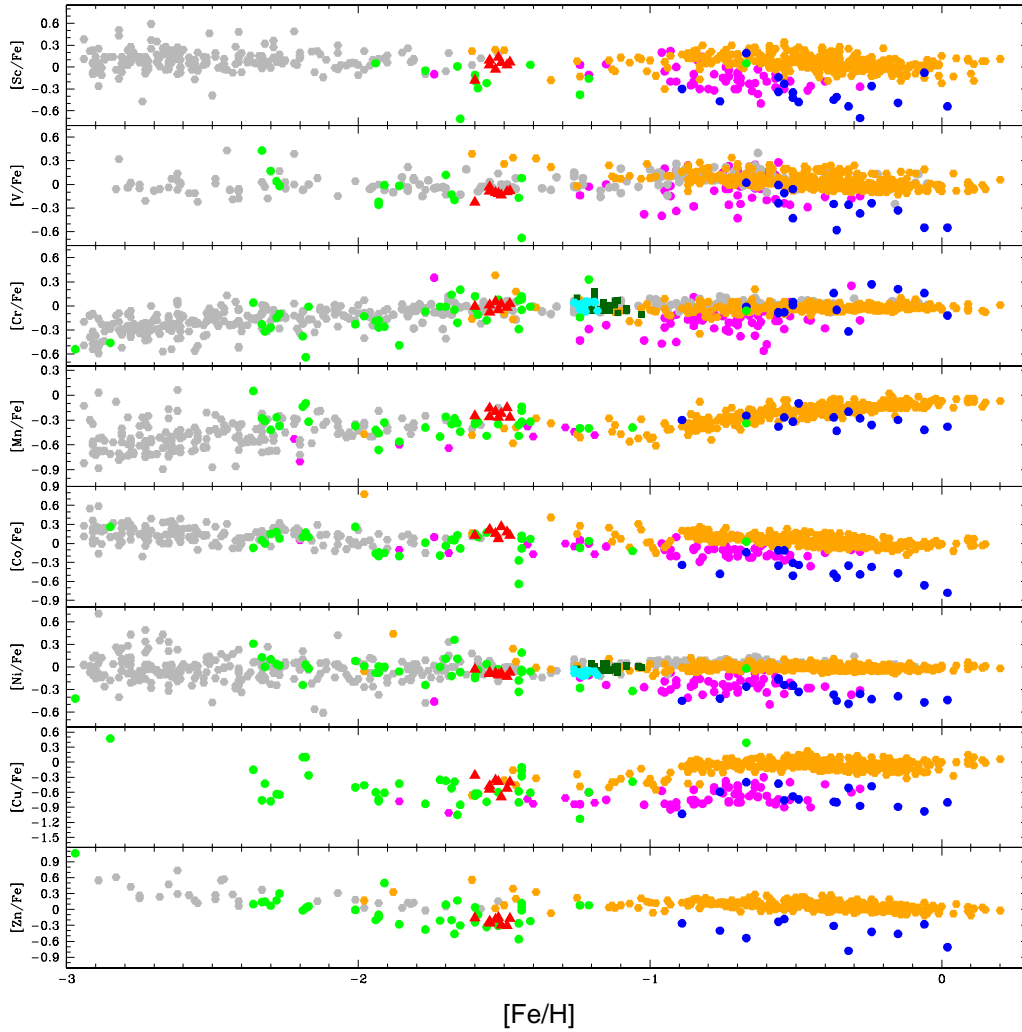


Figure 5. [Sc/Fe], [V/Fe], [Cr/Fe], [Mn/Fe], [Co/Fe], [Ni/Fe], [Cu/Fe], [Zn/Fe] vs [Fe/H]. Filled red triangles are our data from NGC3201, filled gray circle are halo stars from Fulbright (2000) and François et al. (2007)(for all elements, except for [Cu/Fe]), filled orange circle are disk stars from Reddy et al. (2003, 2006), filled green circle are Draco, Sextans and Ursa minor stars from Shetrone et al. (2001), filled magenta circle are LMC stars (for all elements, except for [Mn/Fe] and [Zn/Fe]) from Pompéia et al. (2008), filled blue circle are Sagittarius stars from Sbordone et al. (2007), filled dark green squares is M4 for [Cr/Fe] and [Ni/Fe] from Villanova & Geisler (2011) and filled cyan circle is NGC1851 for [Cr/Fe] and [Ni/Fe] from Villanova, Geisler & Piotto et al. (2010).

Table 1. Basic parameters of the observed stars.

N°	NOMAD ID	Ra (h:m:s)	DEC ($^{\circ}$:':")	B (mag)	V (mag)	J (mag)	K (mag)	RV_H (km/s)	T_{eff} (K)	log(g) (dex)	v_t (km/s)	[Fe/H]
1	0436-0223885	10:18:15.8	-46:21:51.2	14.800	13.430	10.657	9.817	493.57	4480	1.13	1.49	-1.51
2	0435-0223784	10:16:51.7	-46:25:22.6	14.070	12.830	10.421	9.592	492.85	4410	0.92	1.58	-1.53
3	0435-0223980	10:16:59.2	-46:24:11.1	14.050	12.740	10.285	9.432	491.57	4330	0.60	1.55	-1.60
4	0436-0222665	10:17:38.1	-46:22:39.2	14.120	12.690	9.928	9.028	495.60	4290	0.94	1.64	-1.48
5	0435-0225585	10:17:42.5	-46:27:15.4	14.010	12.530	9.757	8.859	497.90	4280	0.72	1.71	-1.49
6	0435-0225390	10:17:38.6	-46:27:16.0	14.020	12.470	9.586	8.650	496.64	4175	0.45	1.76	-1.55
7	0436-0222791	10:17:41.5	-46:20:51.1	13.870	12.300	9.571	8.663	497.53	4182	0.62	1.74	-1.52
8	0436-0222622	10:17:36.9	-46:23:12.0	13.910	12.430	9.599	8.692	495.74	4210	0.65	1.68	-1.55

Table 2. Columns 2-9: abundances of the observed stars. Column 10: mean abundance for the cluster. Column 11: abundances adopted for the Sun in this paper. Abundances for the Sun are indicated as $\log\epsilon(\text{El.})$.

El.	1	2	3	4	5	6	7	8	Cluster ¹	Sun
[C/Fe]	-0.97	-0.76	-0.34	-0.35	-0.40	-0.90	-0.43	-0.62	-0.60±0.09	8.49
[N/Fe]	1.09	0.98	0.31	0.29	-0.05	0.53	0.46	0.77	+0.55±0.13	7.95
[O/Fe]	-0.36	-0.16	0.15	0.40	0.27	0.37	0.25	0.11	+0.13±0.09	8.83
[CNO/Fe]	0.14	0.13	0.09	0.29	0.15	0.27	0.18	0.15	+0.18±0.02	9.01
[Na/Fe] _{NLTE}	0.6	0.45	-0.35	-0.2	-0.25	-0.05	0.05	0.28	+0.07±0.12	6.32
[Mg/Fe]	0.28	0.25	0.54	0.41	0.38	0.34	0.44	0.37	+0.38±0.03	7.56
[Al/Fe]	0.92	0.93	0.36	0.19	0.15	0.14	0.20	0.63	+0.44±0.12	6.43
[Si/Fe]	0.23	0.27	0.12	0.22	0.25	0.27	0.34	0.29	+0.25±0.02	7.61
[Ca/Fe]	0.31	0.31	0.40	0.25	0.33	0.30	0.33	0.33	+0.32±0.01	6.39
[Sc/Fe]	0.06	-0.03	-0.18	0.07	0.03	0.03	0.13	0.09	+0.03±0.04	3.12
[Ti/Fe] ²	0.22	0.26	0.28	0.30	0.22	0.27	0.23	0.24	+0.25±0.01	4.94
[V/Fe]	-0.14	-0.11	-0.23	-0.08	-0.10	-0.04	-0.12	-0.09	-0.11±0.02	4.00
[CrI/Fe]	0.02	0.05	-0.01	0.03	-0.02	0.01	-0.05	-0.08	-0.01±0.01	5.63
[Mn/Fe]	-0.22	-0.20	-0.25	-0.27	-0.15	-0.16	-0.27	-0.26	-0.22±0.02	5.37
[Fe/H]	-1.51	-1.53	-1.60	-1.48	-1.49	-1.55	-1.52	-1.55	-1.53±0.01	7.50
[Co/Fe]	0.26	0.16	0.13	0.13	0.18	0.21	0.07	0.22	+0.17±0.02	4.93
[Ni/Fe]	-0.08	-0.08	-0.03	-0.07	-0.13	-0.09	-0.11	-0.07	-0.08±0.01	6.26
[Cu/Fe]	-0.69	-0.36	-0.26	-0.4	-0.52	-0.47	-0.39	-0.54	-0.45±0.05	4.19
[Zn/Fe]	-0.30	-0.19	-0.16	-0.17	-0.31	-0.26	-0.15	-0.22	-0.22±0.02	4.61
[Y/Fe]	-0.19	-0.15	-0.28	-0.14	-0.21	-0.10	-0.11	-0.11	-0.16±0.02	2.25
[Zr/Fe]	0.19	0.21	0.23	0.43	0.17	0.27	0.16	0.31	+0.25±0.03	2.56
[Ba/Fe]	0.12	0.15	0.07	0.19	0.13	0.08	0.14	0.13	+0.13±0.01	2.34
[La/Fe]	0.07	0.01	-0.11	-0.01	0.02	0.14	0.09	0.09	+0.04±0.03	1.26
[Ce/Fe]	-0.29	-0.16	-0.24	0.06	-0.18	-0.22	-0.21	-0.07	-0.16±0.04	1.53
[Pr/Fe]	0.19	0.19	0.07	0.37	0.17	0.23	0.32	0.23	+0.22±0.03	0.71
[Nd/Fe]	0.13	0.12	-0.12	0.31	0.16	0.21	0.25	0.19	+0.16±0.05	1.59
[Sm/Fe]	0.18	0.21	0.17	0.46	0.28	0.31	0.21	0.30	+0.27±0.04	0.96
[Eu/Fe]	0.28	0.33	0.25	0.51	0.41	0.39	0.44	0.38	+0.37±0.03	0.52
[Dy/Fe]	-0.15	0.2	-	0.57	-0.04	-0.22	0.01	-0.4	0.00±0.12	1.10
[Pb/Fe]	-	0.03	0.26	0.31	-0.13	-0.11	-0.09	0.21	+0.07±0.07	1.98

¹ The errors are statistical errors obtained of the mean.² [Ti/Fe] is the average between Ti I and Ti II.

to our data.

We further investigate any potential metal spread in our sample by comparing stars #3 and #4 of our sample. Both stars have a similar temperature and the most significant difference in [Fe/H], 0.12 dex. Figure 4 shows the star more metal-poor in black and the more metal-rich in red, both spectral lines are Fe. There is a difference in the depth of the lines, which could be attributed to an intrinsic spread, as found by Simmerer et al. (2013). Also in the Figure 4 we compare a pair of stars with similar Fe abundance and temperature, these do not show any difference in the depth of these lines. On the other hand star #3 is the only star of our sample that shows this difference, therefore our result is not conclusive. We cannot rule out a variation on the order of 0.12 dex.

Although there is evidence for an intrinsic spread of iron in NGC3201, mainly found by Simmerer et al. (2013), this needs to be studied in more detail. Because so far, only the more massive GCs have shown a larger spread in iron (Caretta et al. 2009c). However, NGC3201 is among the less massive halo clusters.

The chemical abundances for the Iron-peak elements Sc, V, Cr, Mn, Co, Ni, Cu and Zn listed in Table 2 are solar scaled or slightly underabundant in the cases of Mn, Zn and especially Cu. Figure 5 shows each of our stars in each of

these elements compared with results for the halo field stars, disk stars, other GCs, LMC stars, dSphs, etc. In general, we found that NGC 3201 stars have abundances of these elements which agree with those of other GCs and halo field stars of similar metallicity. All elements, with the possible exception of V, are consistent with no intrinsic dispersion.

Our only strongly non-solar Fe-peak element is Cu, with a value of [Cu/Fe] = -0.45 ± 0.05 . The origin of Cu has been discussed by several authors (Matteucci et al. 1993; Raiteri et al. 1993; Sneden et al. 1991). It can be produced by different nucleosynthetic processes and it is, therefore, difficult to give a definitive explanation of the origin of this element in GCs.

Sneden et al. (1991) suggests that the formation of Cu took place as a weak component of the s-process in massive stars. Matteucci et al. (1993) and Raiteri et al. (1993) suggest that a strong contribution of Cu comes from SNeIa. Therefore, Cu could be a good indicator of the pollution due to the SNeIa to the cluster.

When analyzing the possible origin of Cu in NGC3201, we found that there is no significant correlation between Cu and weak-s component elements (Y, Zr) nor between Cu and main-s components (Ba). Therefore, we can rule out a significant contribution of these processes to the nucleosynthesis of Cu. On the other hand, given the low abundance of Cu and Zn (the next heavier element), the low spread in both

Table 3. Estimated errors on abundances, due to errors on atmospheric parameters and to spectral noise, compared with the observed errors.

ID	$\Delta T_{eff} = 40K$	$\Delta \log(g) = 0.14$	$\Delta v_t = 0.02$	$\Delta [Fe/H] = 0.04$	S/N	σ_{tot}	σ_{obs}
$\Delta([C/Fe])$	-0.06	-0.03	-0.01	0.01	0.04	0.08	0.25
$\Delta([N/Fe])$	-0.06	-0.01	-0.05	-0.01	0.04	0.09	0.38
$\Delta([O/Fe])$	-0.02	0.05	0.01	0.04	0.05	0.08	0.26
$\Delta([Na/Fe])$	-0.02	-0.01	0.00	0.01	0.04	0.04	0.35
$\Delta([Mg/Fe])$	-0.03	0.03	0.00	0.01	0.04	0.06	0.07
$\Delta([Al/Fe])$	-0.01	-0.02	0.04	0.02	0.03	0.06	0.34
$\Delta([Si/Fe])$	0.01	-0.07	0.00	0.00	0.05	0.09	0.06
$\Delta([Ca/Fe])$	0.00	-0.03	-0.01	-0.01	0.04	0.05	0.04
$\Delta([Sc/Fe])$	0.02	-0.05	-0.01	0.01	0.05	0.07	0.10
$\Delta([Ti/Fe])$	0.03	-0.02	0.00	-0.01	0.02	0.04	0.05
$\Delta([TiII/Fe])$	-0.05	0.04	-0.01	-0.01	0.09	0.11	0.06
$\Delta([V/Fe])$	-0.01	-0.02	0.01	0.03	0.03	0.05	0.06
$\Delta([CrI/Fe])$	0.03	-0.02	-0.01	-0.01	0.03	0.05	0.04
$\Delta([Mn/Fe])$	0.00	-0.02	0.00	-0.01	0.04	0.05	0.05
$\Delta([Fe/H])$	0.05	0.01	0.00	0.00	0.01	0.05	0.04
$\Delta([Co/Fe])$	0.02	0.00	-0.01	-0.02	0.04	0.05	0.06
$\Delta([NiI/Fe])$	-0.01	0.00	0.00	0.00	0.02	0.02	0.03
$\Delta([Cu/Fe])$	-0.04	-0.02	0.00	-0.03	0.04	0.07	0.13
$\Delta([Zn/Fe])$	-0.01	0.03	0.02	0.06	0.04	0.08	0.06
$\Delta([Y/Fe])$	0.01	0.03	-0.02	0.00	0.04	0.05	0.06
$\Delta([Zr/Fe])$	-0.05	0.06	0.01	0.01	0.03	0.08	0.09
$\Delta([Ba/Fe])$	-0.05	0.06	0.00	0.01	0.04	0.09	0.04
$\Delta([La/Fe])$	-0.03	0.04	0.00	0.01	0.04	0.06	0.08
$\Delta([Ce/Fe])$	-0.01	0.03	0.00	0.02	0.05	0.06	0.11
$\Delta([Pr/Fe])$	-0.01	0.02	-0.01	0.00	0.04	0.05	0.09
$\Delta([Nd/Fe])$	-0.06	0.04	-0.03	0.00	0.04	0.09	0.13
$\Delta([Sm/Fe])$	0.01	0.01	0.00	0.02	0.04	0.05	0.10
$\Delta([Eu/Fe])$	-0.06	0.06	0.00	0.01	0.04	0.09	0.09
$\Delta([Dy/Fe])$	-0.03	0.05	0.01	0.02	0.04	0.07	0.32
$\Delta([Pb/Fe])$	-0.19	-0.17	-0.18	-0.10	0.04	0.33	0.19

and the overabundance of the alpha elements, we suggest a low contribution of SNeIa to NGC3201.

4.2 α elements

All the α elements (O, Mg, Si, Ca and Ti) listed in Table 2 are overabundant. This is typical of almost every GC as well as similarly metal-poor halo field stars in the Galaxy, as shown in Figure 13. This is our first strong chemical suggestion that NGC 3201 may NOT have an extraGalactic origin, or that at least its chemical evolution has been very similar to that of other GCs.

If we leave out O (due to its involvement in the Na:O anticorrelation addressed below) and use only Mg, Si, Ca and Ti, we derive a mean α element abundance for NGC3201 of

$$[\alpha/Fe]=0.30 \pm 0.06$$

There is good agreement between σ_{tot} and σ_{obs} , and we conclude that there is no evidence of any internal spread in the α elements. Our mean value is in good agreement with Gonzalez & Wallerstein (1998), who found $[\alpha/Fe] = 0.36 \pm 0.09$, and Carretta et al. (2009a, 2010a), who found a mean value of $[(Mg+Ca+Si)/Fe] = 0.31 \pm 0.02$.

Virtually all GGCs show a similar overabundance of the alpha elements, as shown in Figures 12 and 13. This behavior is due to the contribution of high-mass stars that end their lives as SNeII, which are very efficient in enriching the inter-

stellar medium with alpha elements (Tinsley 1979; Sneden 2004).

From Figure 13 we notice that GGCs (in blue) for Mg, Si, Ti and specially Ca show a very strong trend, in each case NGC3201 follows the same trend.

If we consider the following points about the α elements, it is possible to understand their behavior in NGC3201 :

- Proton-capture nucleosynthesis can affect the abundance of Mg, but this element shows no significant spread, although Al does.
- Ti can be affected by other nucleosynthetic processes, but this element also shows no significant spread.
- The main source of α -elements are SNeII, and the pure alpha-elements are Ca and Si.
- The mean abundance we find for pure alpha-elements is $[(Ca+Si)/Fe]=0.29$, which is consistent with the value of all alpha elements (Mg, Si, Ca and Ti).

The enhanced $[\alpha/Fe]$ ratio we find in NGC 3201, closely mimicking values found in other Galactic halo tracers, indicates that it also experienced rapid chemical evolution dominated by SNeII. This strongly suggests that its chemical enrichment was very similar if not identical to that experienced in these other halo objects and was not like that of dSphs, which experienced much slower chemical evolution, leading to low and even subsolar $[\alpha/Fe]$ ratios at low metallicity (e.g. Geisler et al. 2007).

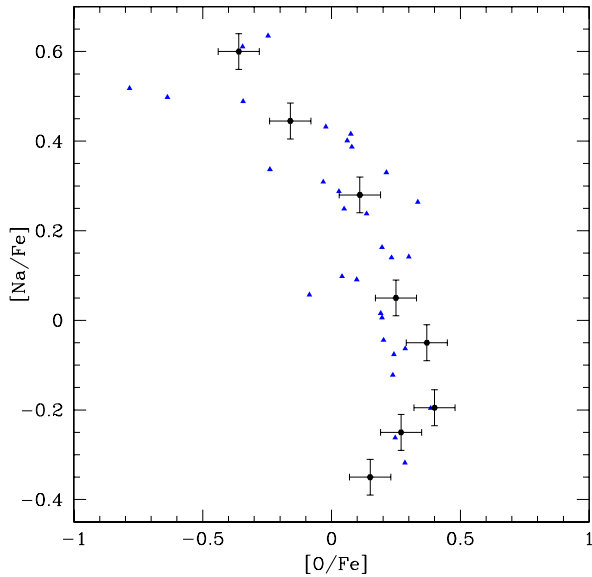


Figure 6. Na-O anticorrelation for NGC3201. Filled black circles with error bars are our data. Filled blue triangles are data from Carretta et al. (2009b).

4.3 Na-O anticorrelation

The anticorrelation between Na and O has been very well established and studied in many GCs, including NGC 3201. Both Gonzalez & Wallerstein (1998) and Carretta et al. (2009b) have in fact already established this anticorrelation in our cluster. We completely corroborate their findings. In Figure 6 our data appear together with those of Carretta et al. (2009b). Very good agreement occurs between them.

Carretta et al. (2009a) found spreads in O and Na very similar to ours: $\sigma_{obsCarretta}[O/Fe] = 0.28$ and $\sigma_{obsCarretta}[Na/Fe] = 0.31$. The dispersion in [O/Fe] and especially [Na/Fe] is one of the highest among the 19 GCs studied by Carretta et al. (2009a), comparable to those in NGC1904, NGC2808 and NGC6752.

Carretta et al. (2007) found a strong relation between Na-O extension and the extension of the HBs, in agreement with D’Antona et al. (2002) prediction. In the case of NGC3201 it shows an extended Na-O anticorrelation with a well populate and extended HB.

Our data do suggest a curious trend for the most Na-poor stars to actually show a small Na:O correlation, but this is based on only three stars and is very preliminary.

Our sample suggests stars of the first generation, generally believed to be those lowest in [Na/Fe] and highest in [O/Fe], have abundances for both of these elements relatively low compared with the other GCs from Carretta et al. (2009a). This could indicate that NGC 3201 formed in an environment with exceptionally low Na and O for its metallicity compared to other GCs, a hint in favor of an extraGalactic origin, but more data are needed to clarify this issue, as we have only one star (star #3) which is very Na poor. An example of the spectral fit to Na in star #3 is given in Figure 7.

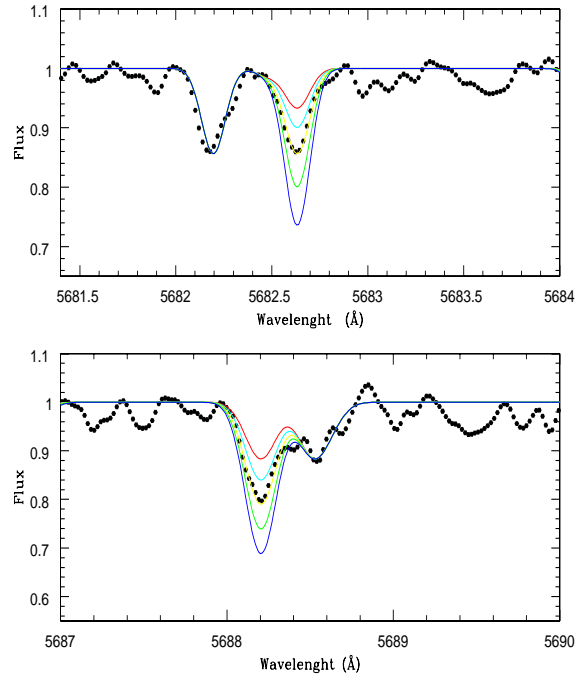


Figure 7. Spectrum synthesis fits for two lines of Na in the star #3 from NGC3201. The solid color lines show the synthesized spectra corresponding to different abundances of Na ([Na/Fe]=0.12, -0.08, -0.32, -0.47, -0.67).

4.4 Mg-Al anti-correlation

A Mg-Al anticorrelation is also found in some GCs (Carretta et al. 2009a). However, unlike the O-Na anticorrelation, a Mg-Al anticorrelation is more difficult to reproduce in simulations and it remains a puzzle to explain the possible sources that would produce this anticorrelation (Denisenkov et al. 1998; Yong et al. 2003).

NGC3201 exhibits a curious behavior in this regard. Our sample has a significant spread in Al ($\sigma_{obs} = 0.34 \pm 0.12$) but no significant spread in Mg ($\sigma_{obs} = 0.08 \pm 0.03$), Figure 10 shows our data together with data from Carretta et al. (2009a) and Gonzalez & Wallerstein (1998). Although the observed range in Mg abundance is only slightly larger than that expected from observational errors, one could imagine a behavior in this diagram similar to that hinted at in the Na:O diagram, in which the stars with the smallest [Al/Fe] abundances exhibit a suggestion of a correlation, followed by a possible anticorrelation for the most [Al/Fe] enhanced stars.

The possible “correlation” seen in the first stars in NGC3201 is similar to the behavior displayed by disk and halo field stars. A shift to a weak anticorrelation in NGC3201 appears to occur approximately at the maximum value for Mg and Al reached by stars in the halo and the disk, although the NGC 3201 sample are generally displaced to smaller [Al/Fe] values at the same [Mg/Fe]. Although the explanation for this behavior is not clear, it supports the possibility of a Galactic origin for NGC3201.

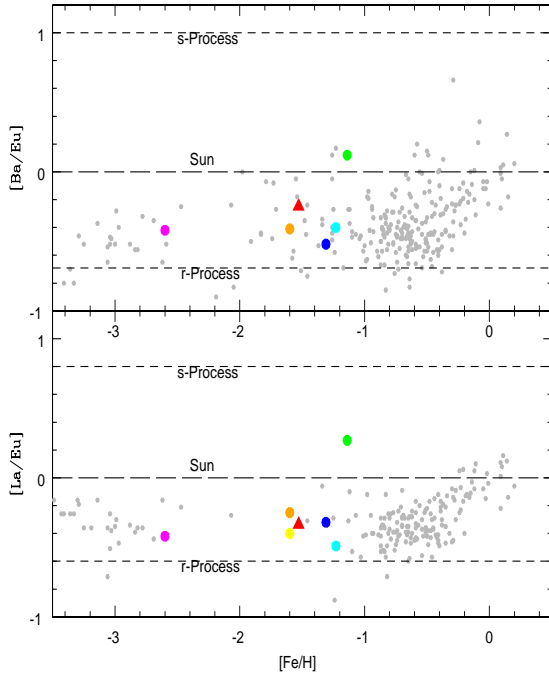


Figure 8. [Ba/Eu] and [La/Eu] vs [Fe/H]. The filled red triangle is our mean for NGC 3201. Filled gray circles are halo and disk stars from Fulbright (2000) and François et al. (2007). The green circle is M4 (Yong et al. 2008); the magenta circle is M15 (Sobeck et al. 2011); the blue circle is M5 (Yong et al. 2008); the orange circle is NGC6752 and the yellow circle is M13 from Yong et al. (2006) and the cyan circle is NGC1851 from Villanova, Geisler & Piotto et al. (2010).

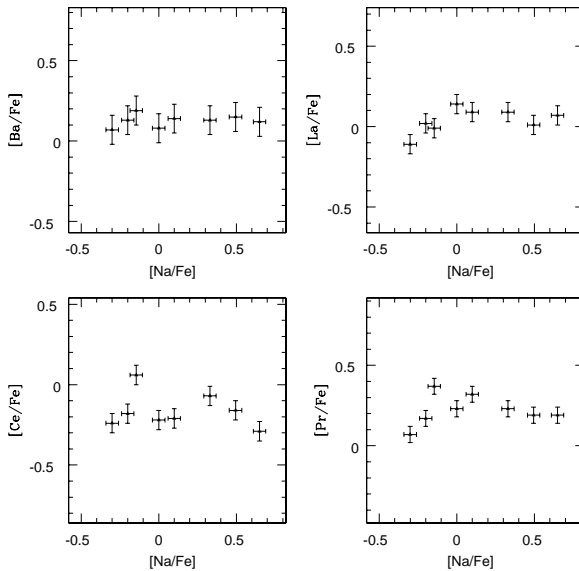


Figure 9. Upper panels: [Ba/Fe] and [La/Fe] as a function of [Na/Fe] for our data. Lower panels: [Ce/Fe] and [Pr/Fe] as a function of [Na/Fe] for our data.

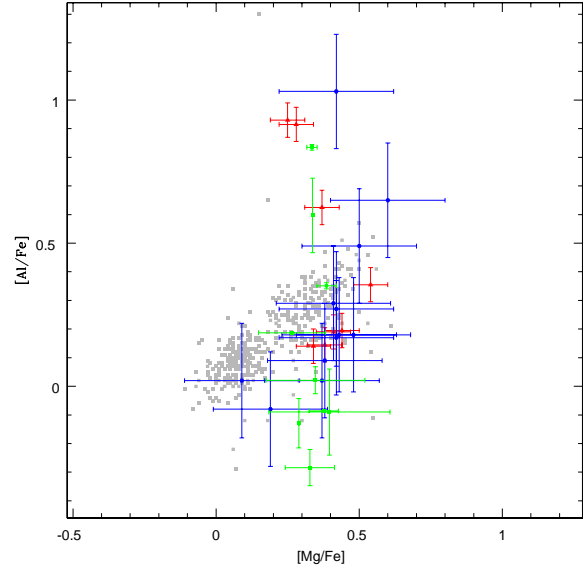


Figure 10. [Mg/Fe] vs [Al/Fe]. Filled red triangles are our data for NGC3201, filled blue circles are data from Gonzalez & Wallerstein (1998) for NGC3201, filled green squares are data from Carretta et al. (2009a) for NGC3201; Filled gray squares are halo and disk field stars from (Fulbright 2000; Reddy et al. 2003; Cayrel et al. 2004; Barklem et al. 2005; Reddy et al. 2006).

4.5 C+N+O and Age

We measured the total (C+N+O) content in NGC3201, obtaining a mean of $[(C+N+O)/Fe]=0.18$ dex, with an insignificant spread.

The total (C+N+O) content has now been measured in several Galactic GCs: M4 stars have $[(C+N+O)/Fe]=+0.29$ dex (Villanova & Geisler 2011), NGC1851 giants show no significant difference in (C+N+O) between the Ba-rich ($[(C+N+O)/Fe]=+0.20$ dex) and Ba-poor ($[(C+N+O)/Fe]=+0.23$ dex) populations (Villanova, Geisler & Piotto et al. 2010) but Yong et al. (2009) found a spread of ~ 0.6 dex in NGC1851. NGC6397, NGC6752 and 47 Tuc also were measured by Carretta et al. (2004) and their stars show a constant (C+N+O) content. NGC3201 stars also display a constant (C+N+O) content. This behavior, apparently, is a trait of the mono-metallic GCs. On the other hand, the GCs non-monometallic show a variation in the content of (C+N+O), e.g. ω Cen shows a correlation between the CNO and their iron content abundance, increasing the $[(C+N+O)/Fe]$ by ~ 0.5 dex between metallicity range from $[Fe/H] \sim -2.0$ to $[Fe/H] \sim -0.9$ (Marino et al. 2012). M22 another non-monometallic cluster shows a similar correlation that ω Cen (Marino et al. 2011b).

The age derived from isochrone fits depends sensitively on (C+N+O) (Cassisi et al. 2008). Marino et al. (2012) found the following relation:

$$\delta \text{ Age} / \delta [(C+N+O)] \sim -3.3 \text{ Gyr/dex}$$

Dotter et al. (2010) derive an age $=12.0 \pm 0.75$ Gyr from a deep HST CMD of NGC 3201 assuming an α -enhanced composition. This age then should be corrected for the ap-

appropriate (C+N+O) abundance we have derived. According to the equation above, the corrected age of NGC3201 is $-3.3 \times 0.18 \sim -0.6$ Gyrs. This brings its age to ~ 11.4 Gyrs. The values used by Dotter et al. (2010) for [Fe/H] and [α /Fe] were only slightly smaller than our values and have a much smaller impact on the derived age.

4.6 Heavy elements

We measured a number of heavy elements (Y, Zr, Ba, La, Ce, Pr, Nd, Sm, Eu, Dy and Pb). These elements are mainly produced by two processes: slow neutron capture reactions (s-process), in which the neutron capture time is much longer than the beta decay lifetime and rapid neutron capture reactions (r-process), where neutron capture times are much shorter than the beta-decay lifetime.

The study of these elements provides the opportunity to better understand these nucleosynthetic processes in GCs. The s-process occurs primarily in AGB stars, producing mainly light-s elements such as Sr, Y, Zr, and heavy-s elements like Ba, whereas massive main sequence stars produce only light s-elements. The r-process occurs mainly in SNeII explosions, producing in particular Eu, along with significant α and iron-peak element enhancements. Thus, studying the detailed heavy element abundances allows us to determine the relative contribution of these processes to the cluster's chemical evolution, in particular during the formation of the second generation, and possibly shedding significant light on this important epoch. The analysis of these elements allows us to investigate the nature of the first generation stars which polluted subsequent generations.

The [Ba/Eu] and [La/Eu] ratios are very sensitive to the relative importance of the s-process vs. r-process. For this purpose, in Figure 8 we plot the abundances of [Ba/Eu] and [La/Eu] vs [Fe/H]. In both cases, we find that these neutron capture elements show a nucleosynthetic history more dominated by the r-process than the s-process. This behavior is also seen in all of the other samples displayed except for M4 and a small sample of disk stars.

The Ba content is constant, with no intrinsic spread, suggesting that AGB stars cannot be a possible polluter, as we should then see the difference between the first and second generations reflected in a spread. This is corroborated by analyzing other heavy s-process elements including La, Ce and Pr (Figure 9), which all show a negligible intrinsic spread. The light s-elements measured by us (Y, Zr) also show no significant spread.

Star #3 has other peculiar features, besides being the most metal poor of our sample (see section 4.1). It also has the lowest values for Y, Ba, La, Pr, ND, Sm, Y and Eu. In some cases their values are very extreme, in particular Y, La and Nd. Some GCs like M22 (Marino et al. 2011b) and NGC1851 (Carretta et al. 2011) have shown similar features, where more iron rich stars are also more neutron-capture rich. This potentially supports the intrinsic spread in Fe in NGC3201 found by Simmerer et al. (2013). On the other hand, in the case of our study we found this feature in only one star of our sample, and although the result is not conclusive it is important to bear in mind.

Another point that is striking is the value of sigma estimated and sigma observed for Dy. The difference is almost 3 sigma, which could be interpreted as a spread of Dy in NCG3201. However, no other neutron capture elements show this spread. Moreover the value in star #4 is unusually high among our sample. Another factor that could affect the measurement of Dy is that the abundance was determined using only one line (5169.688 Å) and this line is very weak. A larger sample of stars with better determined values of Dy would be useful.

5 ANALYSIS OF THE ORIGIN AND CHEMICAL EVOLUTION OF NGC3201

The origin of NGC 3201 is of great interest, not only for its own sake as an intriguing GC but also for helping to understand the origin of the Galactic GC system in general. In particular, we wish to address the Galactic vs. extraGalactic origin of this exotic GC. Additionally, we would like to compare its chemical evolution to that of other GGCs and help constrain scenarios for the generation of MPs.

Kinematically, it is well known that this cluster is an extreme object. It has a very large radial velocity, 495 km s^{-1} , the largest among GGCs. In addition, it has a retrograde orbit. Both of these factors strongly suggest an extraGalactic origin. Rodgers & Paltoglou (1984) and van den Bergh (1993) included it in a list of objects that possibly formed during the merging of the Galaxy with other objects. Allen et al. (2008) studied six globular clusters to determine their galactic orbits (NGC2808, NGC3201, NGC4372, NGC4833, NGC5927, NGC5986) and found that NGC3201 is the least bound to the bar. They showed that its orbit is always outside the bar region using an axisymmetric and the barred potentials representative of our galaxy.

Our analysis, as well as that of both Gonzalez and Carretta before us, has been done from a chemical point of view, adding a distinct dimension to our understanding of the cluster and its possible origin. In particular, we can compare its detailed chemical behavior to that of other objects with a variety of suspected origins. We first replot the Na-O anticorrelation (Figure 11) where we now compare our data (points with error bars) with that of 19 other Galactic GCs (Carretta et al. 2009a,b). In addition, we include LMC objects (Johnson et al. 2006; Pompéia et al. 2008; Mucciarelli et al. 2008), Sagittarius dwarf galaxy field and cluster star (Sbordone et al. 2007), Draco, Sextans and Ursa Minor dwarf galaxy field star (Shetrone et al. 2001).

We can clearly see a region that is only occupied by extraGalactic objects (enclosed by a dashed ellipse) and another region occupied mainly by GGCs (enclosed by a continuous ellipse). The bulk of NGC 3201 giants lie within the Galactic region. However, the trend for the lowest Na stars in NGC 3201 to show a decreased O abundance compared to somewhat higher Na stars is rather unique amongst GGCs, and indeed places these stars, which would generally be considered the likely first generation stars, at the border of the extraGalactic region. Carretta also found stars very poor in Na (Figure 6). These peculiar values among GGCs opens the possibility that the cluster has an extraGalactic origin and subsequently underwent "normal" chemical evolution like typical Galactic GCs, although this is only a rough guess at

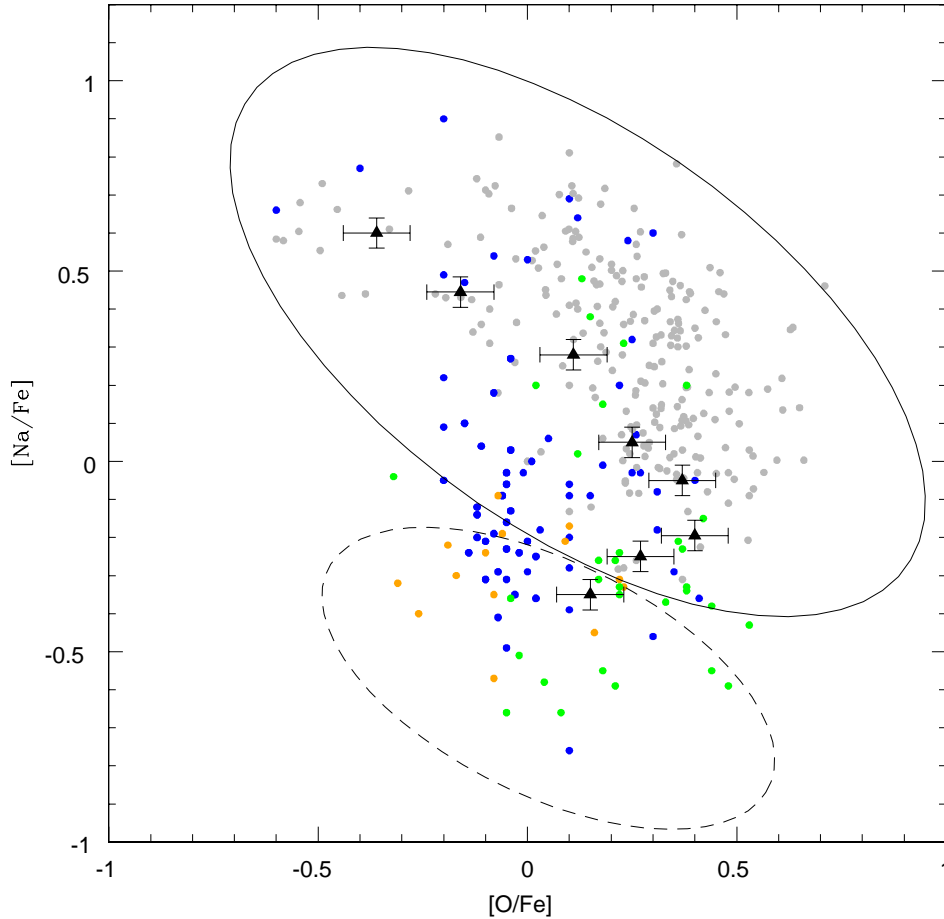


Figure 11. Na-O anticorrelation. Filled black triangles with error bars are our data from NGC3201. Filled gray squares are 19 GCs from Carretta et al. (2009a,b). Blue filled circles are objects from LMC (Johnson et al. 2006; Pompéia et al. 2008; Mucciarelli et al. 2008). Filled orange circles are sagittarius dwarf galaxy (Sbordone et al. 2007). Filled green circle are Draco, Sextans and Ursa minor dwarf galaxies (Shetrone et al. 2001).

this point. Another interesting fact is that NGC 3201 stars display a very large intrinsic spread in both Na and O.

Additional evidence for its origin and evolution comes from the $[\alpha/\text{Fe}]$ vs $[\text{Fe}/\text{H}]$ diagram (Figure 12). Here we include the same objects as in Figure 11, as well as field halo and disk stars (Fulbright 2000; Reddy et al. 2003, 2006). $[\alpha/\text{Fe}]$ was defined as the mean abundance of Mg, Si, Ca and Ti. For LMC’s GCs from Mucciarelli et al. (2009), we used only Mg like a representative value to alpha. For red giant branch stars in Carina dsph galaxy from Lemasle et al. (2012) we used the mean abundance of Mg, Ca and Ti as value to alpha. In the case of GGCs from Carretta et al. (2009a), we added a typical value of Ti for Galactic GCs to obtain the value of $[\alpha/\text{Fe}]$.

In the Figure 12 we again find that Galactic and extraGalactic objects generally occupy different regimes, with some overlap (dashed line in Figure 12 is the galactic trend and solid line is extraGalactic trend). NGC3201’s members fall in the GGC regime but nearer the overlap between galactic and extraGalactic objects than typical GCs. The enhanced $[\alpha/\text{Fe}]$ of NGC 3201 at its metallicity, along with that of

other GCs at other metallicities, graphically illustrates their traditional fast chemical evolution, with both Fe and α elements coming solely from SNeII. Dwarf spheroidal galaxies, on the other hand, had longer star formation time scales, allowing the products of SNeIa to eventually deplete the enhancement of the α elements while continuing to produce additional Fe (e.g. Geisler et al. 2007). The enhanced α abundances, like those in other GCs, argue against a special origin for NGC 3201, although it does appear to be slightly underabundant in the alpha elements than typical GCs at its metallicity. From Figure 13, the underabundance principally stems from Mg and Si, while Ca and Ti appear to be perfectly normal.

From a detailed study of n-capture elements, we found that the abundances of $[\text{La}/\text{Eu}]$ and $[\text{Ba}/\text{Eu}]$ in NGC 3201 are perfectly normal for a halo GC of its $[\text{Fe}/\text{H}]$. The preponderance of the chemical evidence then clearly suggests that NGC 3201 is a normal halo GC, with the only hints of anything strange coming from the behavior of the most Na-poor stars and the behavior from Mg-Al. We conclude that there is no strong chemical reason to support an origin for

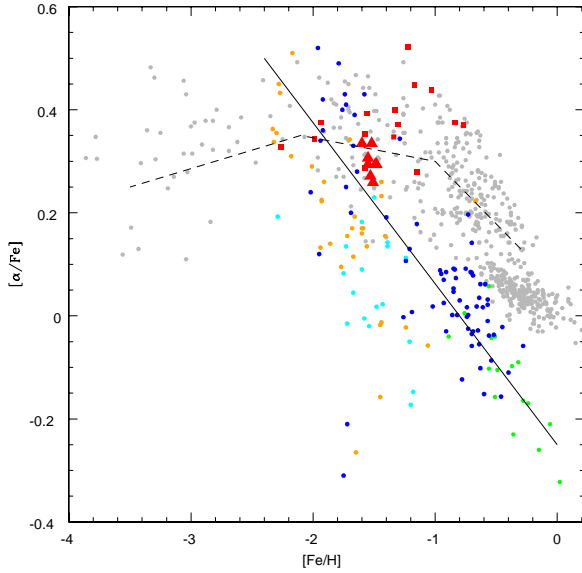


Figure 12. $[\alpha/\text{Fe}]$ vs $[\text{Fe}/\text{H}]$. Filled red triangles are our data from NGC3201. Filled gray circles are halo and disk stars (Fulbright 2000; Cayrel et al. 2004; Reddy et al. 2003, 2006). Filled blue circles are LMC objects (Johnson et al. 2006; Pompéia et al. 2008). Filled red squares are galactic GCs (Carretta et al. 2009a). Filled orange circles are Draco, Sextans and Ursa minor dwarf galaxy (Shetrone et al. 2001). Filled green circles are Sagittarius dwarf galaxy (Sbordone et al. 2007). Filled cyan circles are red giant branch stars in Carina dwarf galaxy (Lemasle et al. 2012).

NGC 3201 that is any different from the bulk of its Galactic counterparts.

On the other hand, it is impossible to ignore the peculiar kinematics of NGC3201. One possible scenario is that it is indeed of extraGalactic origin but was captured very early in its chemical evolution by the MW and subsequently evolved as a typical GGC displaying the typical chemical patterns. Perhaps the low original O and Na abundances are a reminder of its origin. Clearly, although we have shed light on its intriguing nature, there is much left to be learned.

6 SUMMARY AND CONCLUSIONS

In this paper we present detailed chemical abundances of 29 elements in 8 giant members of NGC3201 using high resolution, high S/N spectroscopy. We measure 4 elements using EW and 25 elements using spectral synthesis and perform an accurate error analysis.

We find the following main results:

- NGC 3201 has a mean $[\text{Fe}/\text{H}] = -1.53 \pm 0.01$ with a $\sigma_{\text{obs}} = 0.04$ dex, in good agreement with previous determinations. However, our most metal-poor star may indeed be slightly more metal-poor than the rest. We cannot rule out an intrinsic metal spread of about 0.12 dex.
- We confirm the Na-O anticorrelation. Both of these elements show a very large intrinsic spread compared to the 19 GCs studied by Carretta et al. (2009a,b). We find the most Na-poor stars to also have relatively depleted O abundances,

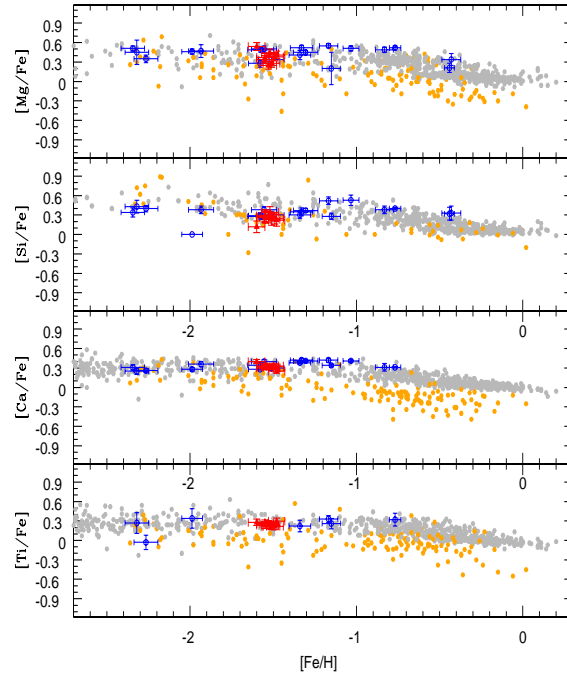


Figure 13. $[\text{Mg}/\text{Fe}], [\text{Si}/\text{Fe}], [\text{Ca}/\text{Fe}], [\text{Ti}/\text{Fe}]$ vs $[\text{Fe}/\text{H}]$. Filled red triangles are giants from NGC3201 from the present study, empty blue circles are GCs (Ivans et al. 2001; Lee et al. 2005; Carretta 2006; Carretta et al. 2009a; Villanova & Geisler 2011; Koch & McWilliam 2011). Filled gray circles are halo and disk stars (Fulbright 2000; Reddy et al. 2003; Cayrel et al. 2004; Barklem et al. 2005; Reddy et al. 2006). Filled orange circles are extraGalactic objects Draco, Sextans, Ursa minor and Sagittarius dwarf galaxy (Shetrone et al. 2001; Sbordone et al. 2007).

hinting that NGC3201 was born in an environment poor in Na.

- Intrinsic spreads are also seen in the light elements C, N, and Al but NOT Mg.
- The Fe-peak elements generally show good agreement with other GCs and halo field stars, with no dispersion.
- A low Cu abundance together with a normal enhancement of the alpha elements likely indicates only a small contribution of SNeIa to the pollution in the proto GC.
- The alpha elements show the typical overabundance observed in other GCs: $[\alpha/\text{Fe}] = 0.30 \pm 0.06$, indicating similar fast star formation time scales and arguing against an extraGalactic origin for the cluster, although the mean alpha abundance is slightly lower than that of similar metallicity GCs.
- The analysis of n-capture elements confirms a dominant contribution from the r-process.
- The heavy s-process elements like Ba show no significant spread, indicating AGB stars were not the likely polluters of the second generation.
- The total (C+N+O) content is constant, similar to most of the monometallic GCs. We derive a correction of some -0.6 Gyr to the age of NGC 3201 derived assuming an α -enhanced composition, yielding ~ 11.4 Gyr as the corrected value.
- Despite its extreme kinematics, NGC3201 shows no

large chemical differences with respect to other GCs, suggesting its origin is similar to those of other GCs. If it is an extraGalactic object, its chemical evolution was similar to that of other GCs.

ACKNOWLEDGEMENTS

We gratefully acknowledge support from the Chilean BASAL Centro de Excelencia en Astrofísica y Tecnologías Afines (CATA) grant PFB-06/2007.

C. Muñoz is supported by CONICYT(Chile) through Programa Nacional de Becas de Magister 2012 (22121324). We would also like to thank the referee for his valuable comments.

REFERENCES

- Allen, C., Pichardo, B. S., & Moreno, E. 2008, *Revista Mexicana de Astronomía y Astrofísica Conference Series*, 34, 107
- Alonso, A., Arribas, S., & Martínez-Roger, C. 1999, *A&AS*, 140, 261
- Barklem, P. S., Christlieb, N., Beers, T. C., et al. 2005, *A&A*, 439, 129
- Bergemann, M., Hansen, C. J., Bautista, M., & Ruchti, G. 2012, *A&A*, 546, A90
- Caloi, V., & D’Antona, F. 2011, *MNRAS*, 417, 228
- Carretta, E., Gratton, R. G., Bragaglia, A., Bonifacio, P., & Pasquini, L. 2004, *A&A*, 416, 925
- Carretta, E. 2006, *AJ*, 131, 1766
- Carretta, E., Recio-Blanco, A., Gratton, R. G., Piotto, G., & Bragaglia, A. 2007, *ApJ*, 671, L125
- Carretta, E., Bragaglia, A., Gratton, R., & Lucatello, S. 2009a, *A&A*, 505, 139
- Carretta, E., Bragaglia, A., Gratton, R. G., et al. 2009b, *A&A*, 505, 117
- Carretta, E., Bragaglia, A., Gratton, R., D’Orazi, V., & Lucatello, S. 2009c, *A&A*, 508, 695
- Carretta, E., Bragaglia, A., Gratton, R., et al. 2010a, *ApJ*, 712, L21
- Carretta, E., Bragaglia, A., Gratton, R. G., et al. 2010b, *ApJ*, 714, L7
- Carretta, E., Bragaglia, A., Gratton, R. G., et al. 2010c, *A&A*, 516, A55
- Carretta, E., Bragaglia, A., D’Orazi, V., Lucatello, S., & Gratton, R. G. 2010d, *A&A*, 519, A71
- Carretta, E., Lucatello, S., Gratton, R. G., Bragaglia, A., & D’Orazi, V. 2011, *A&A*, 533, A69
- Cassisi, S., Salaris, M., Pietrinferni, A., et al. 2008, *ApJ*, 672, L115
- Cayrel, R., Depagne, E., Spite, M., et al. 2004, *A&A*, 416, 1117
- Cote, P., Welch, D. L., Fischer, P., et al. 1994, *ApJS*, 90, 83
- Cottrell, P. L., & Da Costa, G. S. 1981, *ApJ*, 245, L79
- Covey, K. R., Wallerstein, G., Gonzalez, G., Vanture, A. D., & Suntzeff, N. B. 2003, *PASP*, 115, 819
- D’Antona, F., Caloi, V., Montalbán, J., Ventura, P., & Gratton, R. 2002, *A&A*, 395, 69
- Decressin, T., Meynet, G., Charbonnel, C., Prantzos, N., & Ekström, S. 2007, *A&A*, 464, 1029
- de Mink, S. E., Pols, O. R., Langer, N., & Izzard, R. G. 2010, *IAU Symposium*, 266, 169
- Denissenkov, P. A., Da Costa, G. S., Norris, J. E., & Weiss, A. 1998, *A&A*, 333, 926
- Dotter, A., Sarajedini, A., Anderson, J., et al. 2010, *ApJ*, 708, 698
- François, P., Depagne, E., Hill, V., et al. 2007, *A&A*, 476, 935
- Fulbright, J. P. 2000, *AJ*, 120, 1841
- Geisler, D., Wallerstein, G., Smith, V. V., & Casertti-Dinescu, D. I. 2007, *PASP*, 119, 939
- Gonzalez, G., & Wallerstein, G. 1998, *AJ*, 116, 765
- Hansen, C. J., Bergemann, M., Cescutti, G., et al. 2013, *A&A*, 551, A57
- Harris, W. E. 1996, *AJ*, 112, 1487
- Ivans, I. I., Kraft, R. P., Sneden, C., et al. 2001, *AJ*, 122, 1438
- Johnson, J. A., Ivans, I. I., & Stetson, P. B. 2006, *ApJ*, 640, 801
- Johnson, C. I., Pilachowski, C. A., Simmerer, J., & Schwenk, D. 2008, *ApJ*, 681, 1505
- Koch, A., & McWilliam, A. 2011, *AJ*, 142, 63
- Kravtsov, V., Alcaño, G., Marconi, G., & Alvarado, F. 2009, *A&A*, 497, 371
- Kurucz, R. L. 1970, *SAO Special Report*, 309,
- Layden, A. C., & Sarajedini, A. 2003, *AJ*, 125, 208
- Lee, J.-W., Carney, B. W., & Habgood, M. J. 2005, *AJ*, 129, 251
- Lemasle, B., Hill, V., Tolstoy, E., et al. 2012, *A&A*, 538, A100
- Marcolini, A., Gibson, B. K., Karakas, A. I., & Sánchez-Blázquez, P. 2009, *MNRAS*, 395, 719
- Marino, A. F., Villanova, S., Piotto, G., et al. 2008, *A&A*, 490, 625
- Marino, A. F., Milone, A. P., Piotto, G., et al. 2011a, *ApJ*, 731, 64
- Marino, A. F., Sneden, C., Kraft, R. P., et al. 2011b, *A&A*, 532, A8
- Marino, A. F., Milone, A. P., Piotto, G., et al. 2012, *ApJ*, 746, 14
- Mashonkina, L. I., Shimanskiĭ, V. V., & Sakhbullin, N. A. 2000, *Astronomy Reports*, 44, 790
- Matteucci, F., Raiteri, C. M., Busson, M., Gallino, R., & Gratton, R. 1993, *A&A*, 272, 421
- Mucciarelli, A., Carretta, E., Origlia, L., & Ferraro, F. R. 2008, *AJ*, 136, 375
- Mucciarelli, A., Origlia, L., Ferraro, F. R., & Pancino, E. 2009, *ApJ*, 695, L134
- Pompéia, L., Hill, V., Spite, M., et al. 2008, *A&A*, 480, 379
- Raiteri, C. M., Gallino, R., Busso, M., Neuberger, D., & Kaeppler, F. 1993, *ApJ*, 419, 207
- Reddy, B. E., Tomkin, J., Lambert, D. L., & Allende Prieto, C. 2003, *MNRAS*, 340, 304
- Reddy, B. E., Lambert, D. L., & Allende Prieto, C. 2006, *MNRAS*, 367, 1329
- Rodgers, A. W., & Paltoglou, G. 1984, *ApJ*, 283, L5
- Sbordone, L., Bonifacio, P., Buonanno, R., et al. 2007, *A&A*, 465, 815
- Shetrone, M. D., Côté, P., & Sargent, W. L. W. 2001, *ApJ*, 548, 592
- Simmerer, J., Ivans, I. I., Filler, D., et al. 2013, *ApJ*, 764, L7

- Sneden, C. 1973, ApJ, 184, 839
Sneden, C., Gratton, R. G., & Crocker, D. A. 1991, A&A, 246, 354
Sneden, C. 2004, Mem. Soc. Astron. Italiana, 75, 267
Sobeck, J. S., Kraft, R. P., Sneden, C., et al. 2011, AJ, 141, 175
Tinsley, B. M. 1979, ApJ, 229, 1046
van den Bergh, S. 1993, AJ, 105, 971
Villanova, S., Geisler, D., & Piotto, G. 2010, ApJ, 722, L18
Villanova, S., & Geisler, D. 2011, A&A, 535, A31
von Braun, K., & Mateo, M. 2001, AJ, 121, 1522
Yong, D., Grundahl, F., Lambert, D. L., Nissen, P. E., & Shetrone, M. D. 2003, A&A, 402, 985
Yong, D., Aoki, W., Lambert, D. L., & Paulson, D. B. 2006, ApJ, 639, 918
Yong, D., Lambert, D. L., Paulson, D. B., & Carney, B. W. 2008, ApJ, 673, 854
Yong, D., Grundahl, F., D'Antona, F., et al. 2009, ApJ, 695, L62
Zacharias, N., Monet, D. G., Levine, S. E., et al. 2004, Bulletin of the American Astronomical Society, 36, 1418